ELSEVIER

Thermochimica Acta 314 (1998) 69–77

thermochimica acta

Application of the CALPHAD method to material design

Hiroshi Ohtani[a,*], Kiyohito Ishida[b]

[a] *Center for Interdisciplinary Research, Tohoku University, Aramaki, Aoba-ku, Sendai 980-77, Japan*
[b] *Department of Materials Science, Tohoku University, Sendai 980-77, Japan*

Received 29 April 1997; accepted 8 September 1997

Abstract

The outline of the CALPHAD method, which has been developed to alleviate the difficulty in obtaining phase diagrams by experiments alone, is presented. This method enables calculation of stable and metastable phase equilibria, as well as thermodynamic properties such as activity, enthalpy, driving force, and so on. Some examples of the calculated phase diagrams, obtained by applying the CALPHAD method are reviewed, in connection with the design of their microstructures.

Keywords: Materials development; Phase diagrams; Thermodynamic databases

1. Introduction

The various functions of a material are closely related to the phases and the structures of which the material is composed. Therefore, to develop an excellent material with a maximum level of desired functions, it is essential to formulate a design of the structure in advance. Phase diagrams offer the most basic and important information for the design of such new materials. For an experimental determination of the phase boundaries, the specimens are heated over a sufficiently long time at an intended temperature, so that a sufficiently stable state of equilibrium over the specimens can be achieved. However, the diffusivity of atoms is generally not high enough at temperatures below half the melting point. Therefore, it is not actually possible to experiment on the phase equilibrium below that temperature. On the other hand, special devices for temperature control and atmosphere adjustment are required in experiments conducted at extremely high temperatures. To explain the entire phase diagrams only from the experimental works is rather difficult because of these reasons.

The so-called CALPHAD (calculation of the phase diagrams) method is a technique by which a variety of experimental values concerning the phase boundaries and the thermodynamic properties is analyzed according to an appropriate thermodynamic model and the interaction energies between atoms are evaluated [1]. Phase diagrams outside the experimental range can be calculated based on thermodynamic proof according to this method. Difficulty in extension of the calculated results to higher order systems is much less than that in the case of experimental work, since the essence of the calculation does not change so much between a binary system and a higher order system. It is also advantageous that the metastable phase equilibria or the important thermodynamic factors such as driving force and chemical potential, etc. can be

*Corresponding author. Fax: +81 22 217 5756; e-mail: ohtani@cir.tohoku.ac.jp

0040-6031/98/$19.00
PII S0040-6031(97)00457-7

obtained. However, it should be noted that this technique cannot predict the appearance of a completely new phase of which the thermodynamic function has not been evaluated. The free energy of each phase appearing in an alloy system is often approximated by the regular solution model advocated by Hildebrand [2]. This model is based on the thermodynamic model by Van Laar [3], and Bragg and Williams [4,5]. The superiority of this model lies in its description of the thermodynamic properties even in a considerably complex system because of its simple formalism. The regular solution model has most frequently been adopted in the CALPHAD method for this reason [6]. The sublattice model [7] in which the sublattices are introduced into the regular solution approximation has been also used. This model is characterized by its good description of thermodynamic properties, especially of the ordered structure. However, some inaccuracy is still unavoidable as to the entropy term in these models since short-range ordering is neglected (point approximation). Thus, the cluster variation method (CVM) was proposed in which the entropy term is greatly improved by using an atomic cluster [8], and the application of this model was attempted especially in the order–disorder transition of metals [9]. A large number of thermodynamic models are advocated toward the description of free energy besides those introduced here. However, considering the ease of the expansion into multicomponent systems, the sublattice model is thought to be the most appropriate for calculating phase equilibria of practical materials composed of many elements.

The CALPHAD method has been applied to the development of many materials and the interpretation of interesting phenomena [10–12]. For instance, the development of the ALNICO magnet [13], and Co–Cr thin films for high density magnetic recording media [14] are good examples. In this report, the phase diagrams of three alloy systems which our group has analyzed recently by this technique will be reviewed in connection with structure design.

2. Calculation of phase diagrams of materials

Our group has examined some alloy systems from both an experimental and a thermodynamic point of view and has constructed a thermodynamic database based on the results. An outline of those databases was presented in a previous paper [15]. Here, some interesting alloy systems having recently received much attention are taken up, and their calculated phase diagrams are examined from the standpoint of material design.

2.1. Ni-base superalloys

The microstructures of Ni-base superalloys are usually composed of the γ' ($Ni_3Al : L1_2$) phase, which shows an anomalous flow-stress dependence on temperature. In addition to such traditional superalloys, alloys with β (NiAl : B2) phase in their structure have received attention. Exhibiting very high melting temperature and good resistance to oxidation, this β phase is also an important intermetallic compound as surface coating phase of superalloys. Then, in order to make use of each merit, the development of an alloy with a ($\beta+\gamma'$) two-phase structure is anticipated [16]. In the development of such new alloys, phase diagrams contain important information. Some calculated phase diagrams of the Ni-base superalloys are introduced as follows.

Some results of calculation of the isothermal section diagrams of the Ni–Al–Ti ternary system are shown in Fig. 1. This alloy system is a typical Ni-base superalloy which achieves high strength by dispersion of its fine γ' phase in the γ-phase matrix. Participation of the η ($Ni_3Ti : D0_{24}$) phase and H (Heusler) phase, as well as the γ' and β phases, complicates the phase equilibrium of this alloy system in the compositional range of Ni contents of 50% or more. Therefore, the phase boundaries were measured by using diffusion couples [17], and accurate phase equilibrium was determined at the beginning of the analysis.

Calculated isothermal section diagrams of the Ni–Al–Cr and Ni–Al–Co systems are shown in Figs. 2 and 3, respectively. An addition of Cr and Co to the Ni–Al binary system stabilizes the (γ(fcc)+β) two-phase region, although the ((Cr)+β) field occupies a considerable portion of the phase region in the Ni–Al–Cr system. The two-phase region of (γ(fcc)+β) is not observed with the addition of Ti. The β phase is extremely brittle, and working at low temperatures is almost impossible. Recently, our findings clarified that the coexistence of the β phase with the ductile

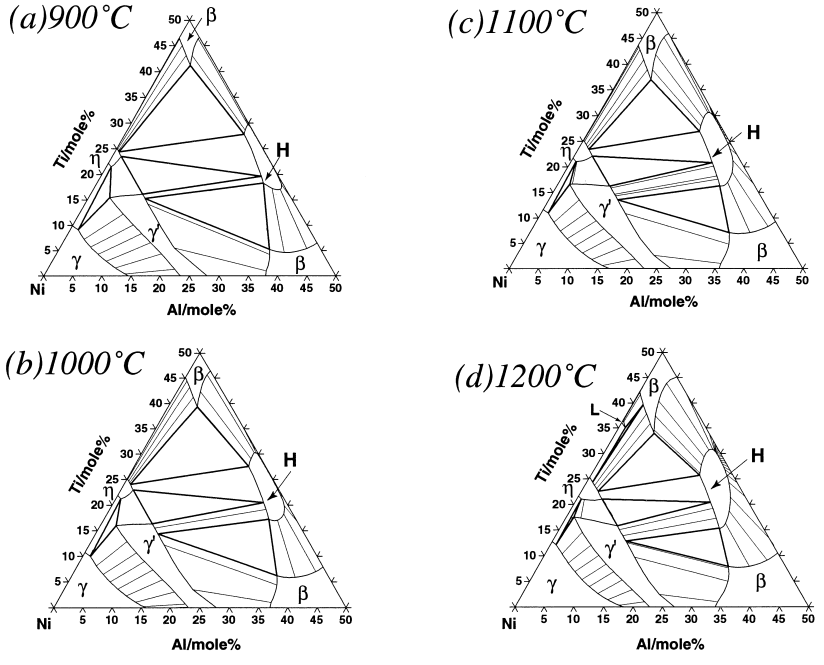

Fig. 1. Calculated isothermal sections of the Ni–Al–Ti ternary system at (a) 900, (b) 1000, (c) 1100, and (d) 1200°C.

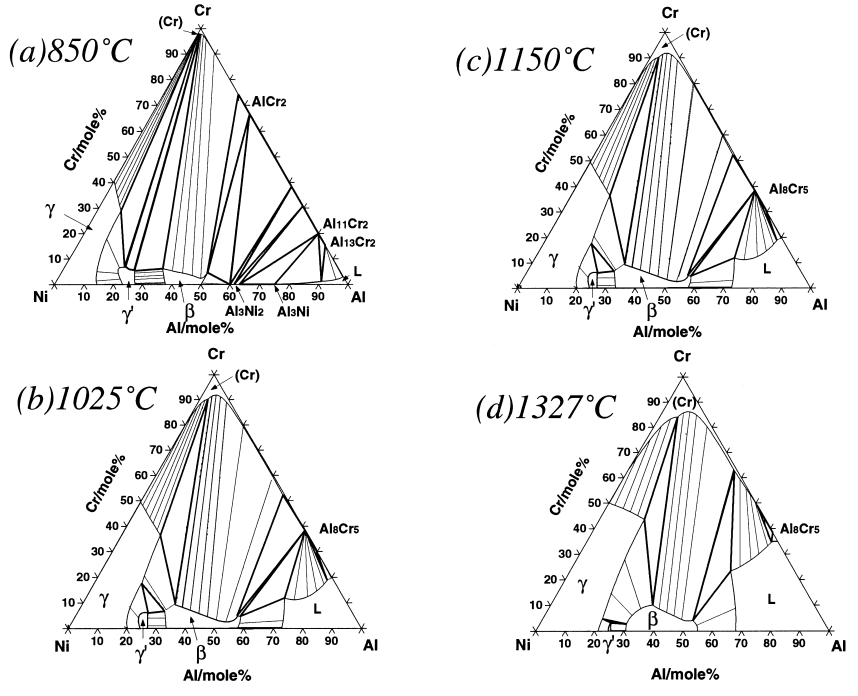

Fig. 2. Calculated isothermal sections of the Ni–Al–Cr ternary system at (a) 850, (b) 1025, (c) 1150, and (d) 1327°C.

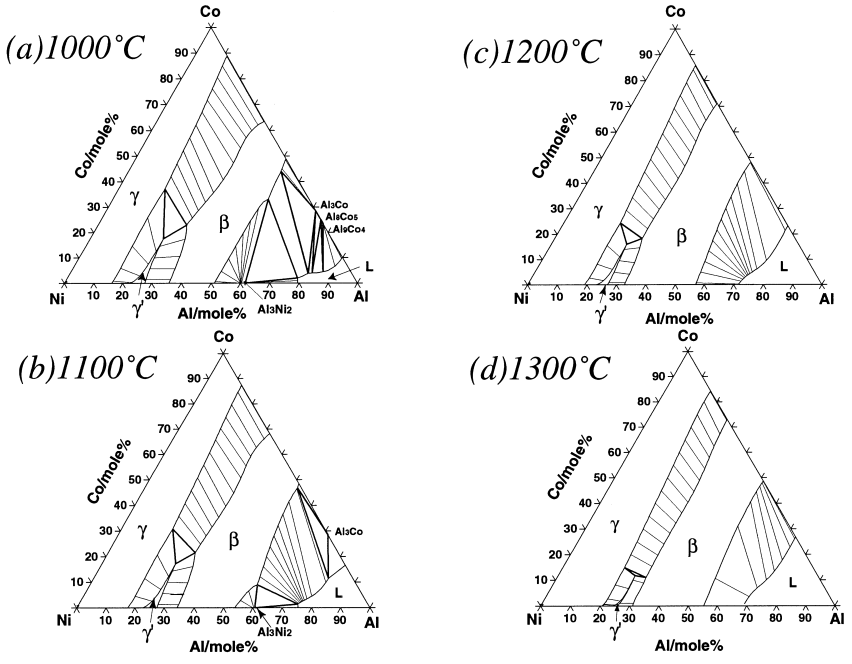

Fig. 3. Calculated isothermal sections of the Ni–Al–Co ternary system at (a) 1000, (b) 1100, (c) 1200, and (d) 1300°C.

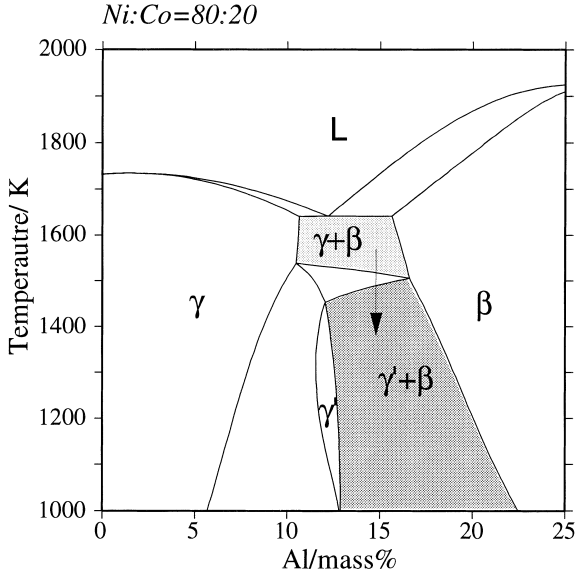

Fig. 4. Vertical section of the Ni–Al–Co ternary system with Ni : Co=80 : 20.

γ(fcc) phase remarkably improves the hot workability of this alloy [16]. However, the high-temperature strength of this alloy may be rather low. This drawback can be improved by replacing this γ phase by the heat-resistant γ′ phase through heat treatment. Fig. 4 shows the vertical section of the Ni–Al–Co ternary system. The development of a heat-resistant alloy with workability can be achieved by the application of processing in the (γ+β) two-phase region at higher temperatures and, subsequently, transforming the γ phase into the γ′ phase at lower temperatures. Such thermomechanical treatments will become possible when the appropriate information based on the calculation of phase diagrams is available. It is extremely difficult to determine such a suitable range of heat treatment only by experiment.

2.2. Microsolder alloys

Pb–Sn eutectic alloy has been employed for microsolder material used in high density mounting of electronic equipment. This alloy is characterized by a low melting point as well as by excellent wettability and connectability. Therefore, it has the merit of being able to limit the influence of heat on electronic devices to a narrow region. However, the methods for connecting semiconductor elements have recently

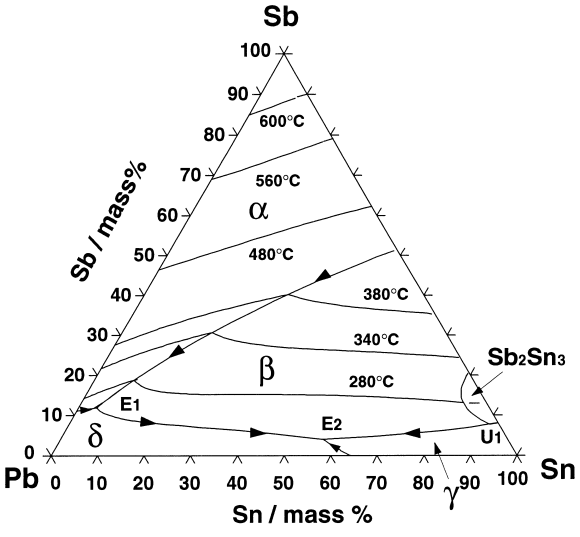

Fig. 5. Calculated liquidus surface of the Pb–Sn–Sb ternary system. E_1, E_2 indicate the ternary eutectic reactions, while U_1 denotes the monotectic reaction.

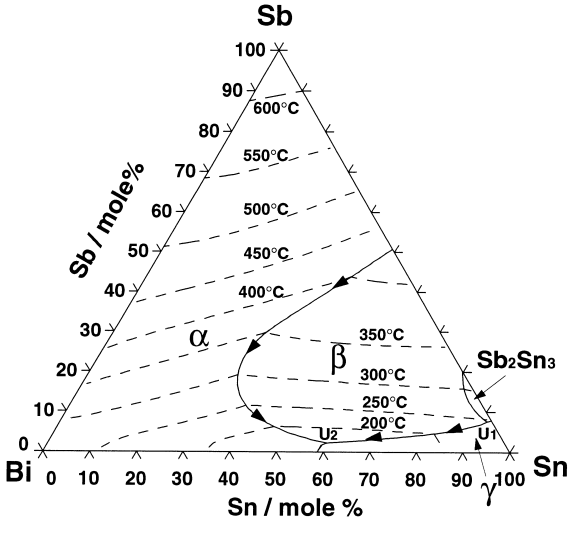

Fig. 6. Calculated liquids surface of the Bi–Sn–Sb ternary system. Two monotectic invariant reactions, indicated by U_1 and U_2 appear.

become diversified. Therefore, in order to deal with new connection technologies such as the controlled-collapse bonding [18], it is insufficient to only use this binary alloy. In addition, the fact that traditional solder contains harmful Pb is also a problem. The use of the solder material which contains Pb is becoming restricted in the United States. It can be easily imagined that such restrictions will also be imposed in other countries in the near future. Thus, the development of multicomponent Pb-free solder alloys with properties comparable to the Pb–Sn binary alloy is urgently required.

We have been systematically examining the phase diagrams of alloy systems composed of Pb, Sn, Sb, Bi, Ag, Zn and Cu. At first, an example of a ternary system based on Pb–Sn is presented. The liquidus surface of the Pb–Sn–Sb ternary system is shown in Fig. 5 [19]. In this ternary system, the surface is composed of the Sb-rich α phase (rhombohedral), the intermetallic β phase (NaCl structure), the Sn-rich γ phase (bct), the Pb-rich δ phase (fcc), and the stoichiometric compound Sb_2Sn_3. No phase peculiar to the ternary system has been reported. Three kinds of invariant reactions take place in the Pb–Sn–Sb ternary system and each reaction is, respectively, indicated by E_1, E_2 (eutectic reaction of both), and U_1 (monotectic reaction) in the figure. E_2 shows the point (179°C) where the melting temperature is the lowest in this ternary system. However, the rate of drop in the melting point from the Pb–Sn binary system is very small. The alloy compositions of practical solder materials concentrate in the neighborhood of this ternary eutectic point E_2.

The development of a new Pb-free solder alloy is being accelerated to avoid water pollution caused by Pb. The Bi–Sn–Sb ternary system is one of the best candidates. It contains the α phase of Bi and Sb (rhombohedral) solution, miscible in all proportions; the intermetallic compound β phase (NaCl structure); the Sn-rich γ phase (bct); the stoichiometric compound Sb_2Sn_3; and the liquid phase. No peculiar phase of this ternary system appears. The liquidus surface of the system is given in Fig. 6 [20]. Since the primary crystal is almost entirely composed of the α and the β phases, as is the case with the Pb–Sn–Sb system, the melting point is comparatively high. This is the reason why this alloy system is generally classified as a solder for use at high temperatures. The ternary eutectic reaction does not take place in the system although two monotectic invariant reactions indicated in the figure by U_1 and U_2 appear. With regard to the use of the Bi–Sn–Sb as a microsolder material, these phase diagrams indicate the range of solidification temperature to be a little too wide, which causes the oxidation and loss of solders by contact with the atmosphere.

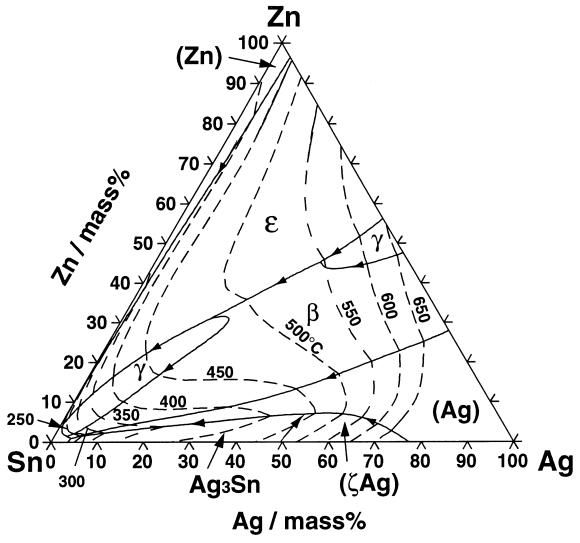

Fig. 7. Calculated liquidus surface of the Sn–Ag–Zn ternary system.

Therefore, it is necessary to improve this aspect by adding alloying elements.

The Sn–Ag–Zn ternary system is also a promising candidate for Pb-free solder. However, little research on phase diagram has been done, and the lack of basic information retards the development of an alloy. From the experimental study by using the X-ray and EDX analysis, the (Ag), (Sn), (Zn), ξAg (hcp), Ag_3Sn (rhombohedral), β (bcc), ξ (hcp), γ (bcc-based ordered structure), ε (hcp) phases in the ternary system were observed; however, no peculiar phase in the ternary system was observed, at least within the range of this experiment. Fig. 7 shows result of calculation of the liquidus surface, which has a gentle peak in the vicinity of the central part of the composition. The ternary eutectic point exists at Sn-4%/Ag-1%/Zn, and the temperature is 216°C. As an alternative alloy of the Pb–Sn system solder, it seems necessary to add a small amount of other low-melting metals in order to further lower the melting point.

The majority of the alloys which are potential Pb-free solders are the Sn-based alloy systems, given the constraints of environment and supply. Sn is an excellent element for electric conductivity, strength, and corrosion resistance. However, as the melting point is too high, it is necessary to control precisely the range of melting point by alloying. Melting point, melting temperature range, and wettability, etc., can be predicted by using the method presented in this paper. Therefore, thermodynamic examination based on the CALPHAD approach is also expected to become important in the development of Pb-free solder alloys.

2.3. Alloy semiconductors

It may not be an exaggeration to say that the device which best represents present-day electronics is the large-scale integrated circuit of Si. Si is a Group IV element and has excellent chemical and mechanical properties, not to mention its electrical properties. On the other hand, alloy semiconductors as optoelectronic material have received much attention in recent years. In particular, Group III–V alloy semiconductors are characterized by high electronic mobility and high luminescence efficiency. To maximize use of its characteristic, the heterojunction has been employed. As a result, an efficient laser diode and receiving light element have been put to practical use, and these devices are essential to present-day communications. To understand the properties of such alloy semiconductors, information contained in phase diagrams is indispensable. For instance, the width of the band gap, which is the most basic wavelength property of optoelectronic devices, is directly related to the homogeneous range of the alloy semiconductors. With this background of such practical use, a thermodynamic database for the groups III–V and II–VI alloy semiconductors has been constructed by the present authors [21,22].

Fig. 8 shows a typical isothermal section diagram of the Group III–V alloy semiconductors. The alloy system shown in Fig. 8 is the In–Ga–Sb system, in which In and Ga of Group III elements mutually substitute for the same sublattice sites in the zinc-blende structure. When an alloy semiconductor is produced by bulk crystal growth and liquid phase epitaxy, knowledge concerning such phase equilibria is very important for the composition control of solid phase, because the solid and liquid phases are in contact at near-equilibrium conditions in these methods. Fig. 9 shows the InSb–GaSb pseudobinary phase diagram of this alloy system. InSb and GaSb form the solid solution, i.e. a mixed crystal, in the lower temperature range and the wavelength of the band

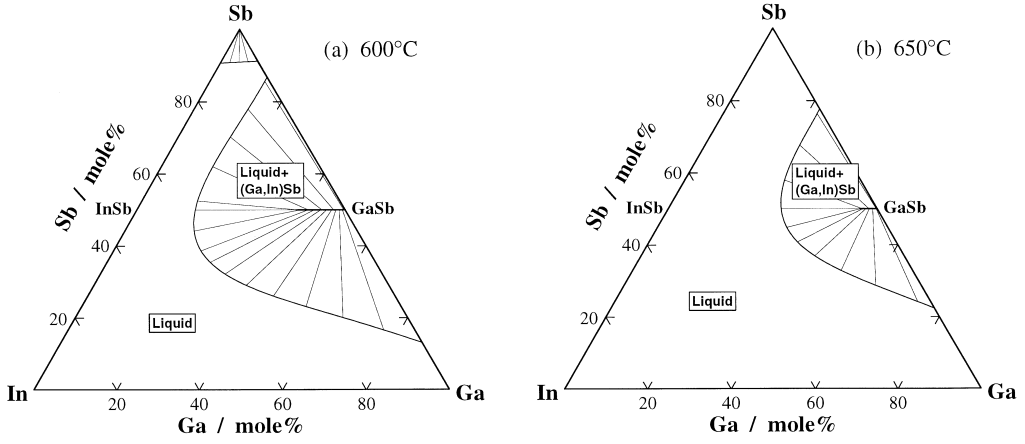

Fig. 8. Isothermal sections of the In–Ga–Sb ternary system at (a) 600 and (b) 650°C.

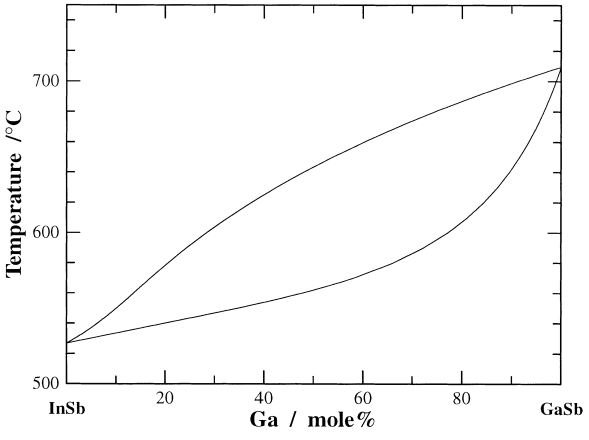

Fig. 9. The calculated phase boundaries of the InSb–GaSb pseudobinary system.

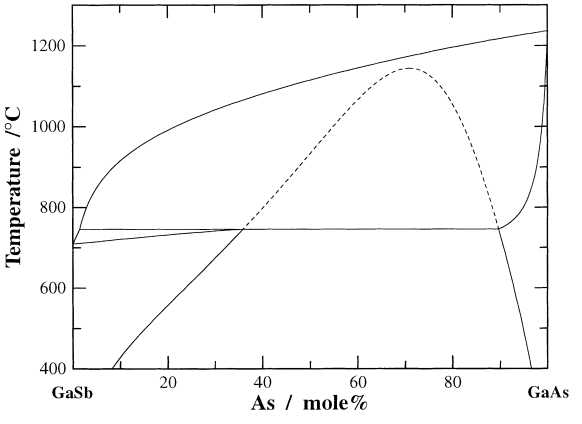

Fig. 10. The calculated phase boundaries of the GaSb–GaAs pseudobinary system.

gap changes remarkably from 1.722 to 6.888 μm, corresponding to the composition.

As given in Fig. 10, there are several alloy systems in which the phase diagrams are peritectic due to two-phase separation of the alloy semiconductors. It is difficult to fabricate an alloy semiconductor by using bulk crystal growth or liquid phase epitaxy because a homogeneous phase is not obtained in such alloy systems. However, it is clear from the calculation that a homogeneous alloy semiconductor can be obtained if the crystal lattice is adjusted to that of a certain substrate. For instance, Fig. 11 shows the result of calculation for the pseudobinary phase diagram when GaAsSb is grown on the InP substrate with (100) plane. In this calculation, the contribution of the lattice mismatch strain to the Gibbs free energy was considered. The top figure is the result when the thickness is 0.1 μm while the bottom figure is the result for 1 μm. The lattice constant lnP is 0.58688 nm, which corresponds to an almost equiatomic composition. A homogeneous solid solution stabilized by the lattice mismatch strain is generated near the composition. It is worthy of note that the thinner the thickness of the growing film is, the more widely such areas appear.

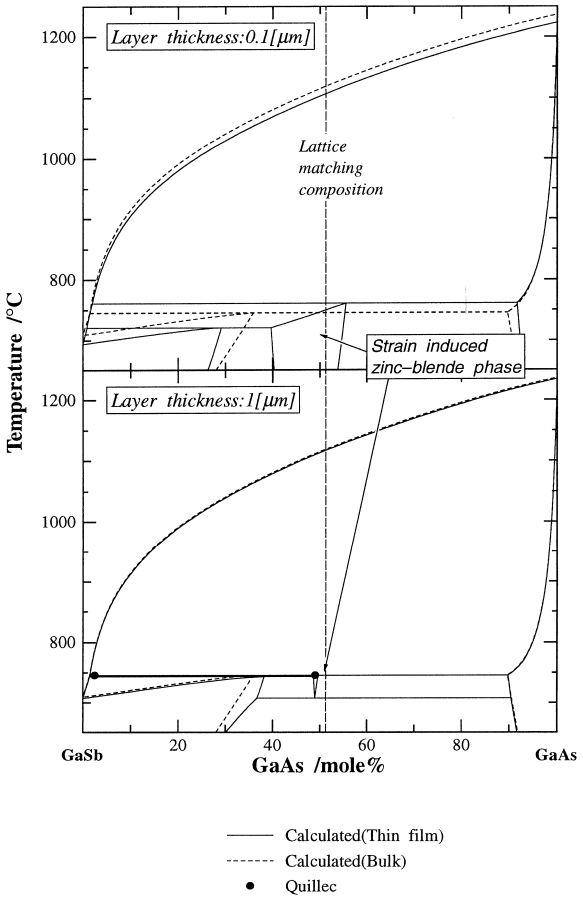

Fig. 11. Calculated phase diagrams of the GaAsSb thin film grown on the InP (100) substrate. The top figure is the result when the layer thickness is 0.1 μm, while the bottom figure is the result for 1 μm.

Quillec et al. [23] investigated the GaAsSb of the thickness of 1 μm growing on the InP substrate and confirmed experimentally that a new solid phase with a composition of 49 mol% appears. This result is shown by filled black circles in the figure. Since the results of calculation and the experimental values agree extremely well as shown, the accuracy of the calculation by using this database is confirmed.

3. Conclusions

The effectiveness of information offered by phase diagrams was discussed from the point of view of material design, in relation to some new materials. The CALPHAD method applied in this paper allows to calculate phase diagrams using an appropriate thermodynamic model. By using this technique, it becomes possible to predict phase equilibria in regions which cannot be accessed experimentally. The merits of using such an approach will be further emphasized in the future with the development of sophisticated calculation software.

Acknowledgements

The authors gratefully acknowledge use of the THERMO-CALC software program for equilibrium phase diagram calculations. This work was supported by the Proposal-Based Advanced Industrial Technology R and D Program, and also by the Grants-in-Aid for Scientific Research from the Ministry of Education, Science, Sports and Culture. The authors also wish to acknowledge the support from the Sumitomo Foundation.

References

[1] T. Nishizawa, Materials Trans. JIM 33 (1992) 713.
[2] J.H. Hildebrand, J. Amer. Chem. Soc. 51 (1929) 66.
[3] J.J. Van Laar, Z. Physik. chem. 63 (1908) 216.
[4] W.L. Bragg, E.J. Williams, Proc. Roy. Soc. A145 (1934) 699.
[5] W.S. Gorsky, Z. Phys. 50 (1928) 64.
[6] L. Kaufman, H. Bernstein, Computer Calculation of Phase Diagram, Acad. Press, NY, 1970.
[7] M. Hillert, L.-I. Staffansson, Acta Chem. Scand. 24 (1970) 3618.
[8] R. Kikuchi, Phys. Rev. 81 (1951) 998.
[9] D. de Fontaine, R. Kikuchi, NBS Publication SP-496 (1978) 999.
[10] F.H. Hayes et al. (Eds.), User Aspects of Phase Diagrams, The Institute of Metals, 1991.
[11] M. Doyama et al. (Eds.), Computer Aided Innovation of New Materials, North-Holland, 1993.
[12] P. Nash, B. Sundman (Eds.), Application of Thermodynamics in the Synthesis and Processing of Materials, TMS, 1995.
[13] S.M. Hao, K. Ishida, T. Nishizawa, Metall. Trans. 16A (1985) 179.
[14] K. Ishida, T. Nishizawa, User Aspects of Phase Diagrams, The Institute of Metals, 1991, p. 185.
[15] H. Ohtani, K. Ishida, T. Nishizawa, Trans. Materials Research Society of Japan 9 (1992) 199.
[16] R. Kainuma, S. Imano, H. Ohtani, K. Ishida, Intermetallics 4 (1996) 37.

[17] C.-C. Jia, K. Ishida, T. Nishizawa, Met. Mat. Trans. 25A (1994) 473.
[18] L.F. Miller, IBM J. Res. Dev., May (1969) 239.
[19] H. Ohtani, K. Okuda, K. Ishida, J. Phase Equilibria 16 (1995) 416.
[20] H. Ohtani, K. Ishida, J. Electr. Materials 23 (1994) 747.
[21] K. Ishida, H. Tokunaka, H. Ohtani, T. Nishizawa, J. Crystal Growth 98 (1989) 140.
[22] H. Ohtani, K. Kojima, K. Ishida, T. Nishizawa, J. Alloys Compounds 182 (1992) 103.
[23] M. Quillec, H. Launois, M.C. Joncour, J. Vac. Sci. Technol. B1(2) (1983) 238.